A highly specific inhibitor of human p38 MAP kinase binds in the ATP pocket

Liang Tong, Susan Pav, Della M. White, Sheri Rogers, Kathy M. Crane, Charles L. Cywin, Maryanne L. Brown and Christopher A. Pargellis

The crystal structure of human p38 mitogen-activated protein (MAP) kinase in complex with a potent and highly specific pyridinyl-imidazole inhibitor has been determined at 2.0 Å resolution. The structure of the kinase, which is in its unphosphorylated state, is similar to that of the closely-related ERK2. The inhibitor molecule is bound in the ATP pocket. A hydrogen bond is made between the pyridyl nitrogen of the inhibitor and the main chain amido nitrogen of residue 109, analogous to the interaction from the N1 atom of ATP. The crystal structure provides possible explanations for the specificity of this class of inhibitors. Other protein kinase inhibitors may achieve their specificity through a similar mechanism. The structure also reveals a possible second binding site for this inhibitor, with currently unknown function.

Mitogen-activated protein kinases (MAP kinases) are crucial components of intracellular signalling cascades that become activated in response to certain extracellular signals such as growth factors (for reviews see refs 1,2). The activation of MAP kinases occurs through the phosphorylation of a Thr and a Tyr residue, in a TXY motif, by the upstream dual-specificity protein kinase in the cascade. To date, three cascades involving MAP kinases have been established. The MAP kinases in these cascades are ERK1/ERK2 (containing a TEY activation motif), p38 (TGY motif), and JNK (TPY motif), respectively. Controlled activation of these cascades by external stimuli can lead to various cellular responses such as proliferation, differentiation and apoptosis, whereas unregulated activation of these cascades can result in oncogenesis.

The crystal structures of Ser/Thr- and Tyr-specific protein kinases show that they contain a conserved catalytic core (for reviews see refs 3,4) that generally consists of a small N-terminal lobe largely composed of an anti-parallel β-sheet, and a large C-terminal lobe which is mostly α-helical. The ATP nucleotide is bound in a deep cleft at the interface between the two lobes[5–10].The phosphate groups of ATP are located near the opening of the cleft, where the substrate also binds. Several highly conserved residues from the C-terminal lobe interact with the γ-phosphate of ATP and provide the catalytic machinery for the kinase reaction. The activation of many protein kinases requires the phosphorylation of residue(s) in an activation segment, which is also located near the opening of this cleft. This phosphorylation controls the conformation of the activation segment, which can in turn regulate the activity of the kinase[3].

The p38 kinase is a newly-identified member of the MAP kinase family[11–15], sharing about 50% sequence identity with the ERKs. It can become activated in response to inflammatory cytokines (such as interleukin-1 and tumour necrosis factor), heat shock, osmotic shock, endotoxin and other signals. This kinase is also the target of a series of pyridinyl-imidazole compounds which suppress the production of inflammatory cytokines[14,16]. These CSAIDs (cytokine-suppressive anti-inflammatory drugs) inhibit the p38 MAP kinase with high specificity and potency (with IC_{50} values in the low nanomolar range) and have little effect on other protein kinases[14,17]. Similar to the ERKs, two highly homologous forms of p38 were identified from human THP.1 cells and were named CSBP1 and CSBP2 (CSAID Binding Protein)[14]. More recently, additional homo-

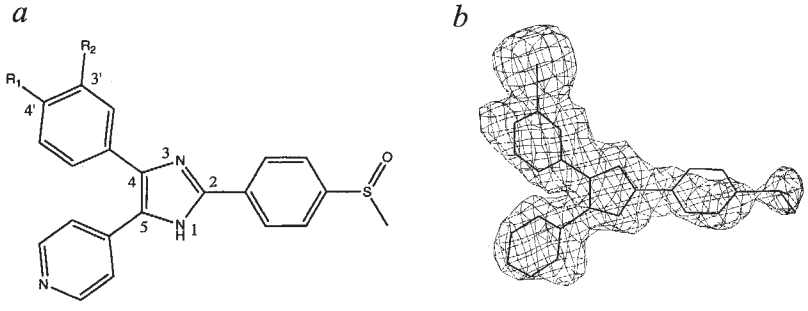

Fig. 1 *a*, The pyridinyl-imidazole inhibitors of p38 MAP kinase used in the current study. The parent compound (R_1=F, R_2=H; SB 203580)[14,17] was modified by introducing an iodine atom at the 3' (R_1=H, R_2=I; 3'-iodo inhibitor) or the 4' (R_1=I, R_2=H; 4'-iodo inhibitor) position. The structure reported here contains the 3'-iodo inhibitor. *b*. Electron density for the 3'-iodo inhibitor molecule in the ATP binding pocket. The map was calculated after simulated-annealing omit refinement against 6.0–2.0 Å resolution data and contoured at 1σ.

Boehringer Ingelheim Pharmaceuticals, Inc., 900 Ridgebury Road, P.O. Box 368, Ridgefield, Connecticut 06877, U.S.A.

Correspondence should be addressed to L.T.
b4w@cc.purdue.edu

Table 1. Summary of data collection and structure refinement

***a*, Data collection**

Crystal	Wavelength	No. of observations	No. of reflections	R_{merge} (%)[1]	Resolution limit (Å)	Completeness (%)
Native	λ3	179632	25456	4.6	2.0	99
Seleno-	λ1	78259	18667[2]	8.0	2.7	91
Methionyl	λ2	78272	18706[2]	8.4	2.7	91
	λ3	78456	18751[2]	8.6	2.7	92
	λ4	78325	18739[2]	8.8	2.7	92

***b*, Structure refinement**

Resolution range	No. of reflections	*R*-factor (%)[3]	No. of inhibitor molecules	No. of waters	R.m.s. bonds (Å)	R.m.s. angles (°)
6.0–2.0 Å	24416	23.4 (30.1)	3	195	0.009	1.6

***c*, Summary of MAD phasing statistics**

From MADSYS

Observed ratios[4] (15–4.0 Å)	λ1	λ2	λ3	λ4	*f'* (e)	*f''*(e)
λ1	0.048 (0.042)	0.046	0.044	0.041	-4.1	0.5
λ2		0.058 (0.042)	0.041	0.047	-10.3	4.0
λ3			0.065 (0.045)	0.044	-8.1	5.0
λ4				0.058 (0.050)	-3.6	4.0

From X-PLOR

Resolution (Å)	5.4	4.3	3.8	3.4	3.2	3.0	2.8	2.7	Overall
<Figure-of-merit>	0.79	0.73	0.68	0.59	0.51	0.45	0.40	0.37	0.58

[1] $R_{merge} = 100 \times \Sigma_h \Sigma_i |I_{hi} - \langle I_h \rangle| / \Sigma_h \Sigma_i I_{hi}$.
[2] The Friedel mates of acentric reflections are kept as separate reflections.
[3] Value in parenthesis is the free *R*-factor[41] for 7.5% of the reflections.
[4] For reflections between 15–2.7 Å resolution, $R(F_A)$ = 49%, $\Delta(\Delta\phi)$ = 52°. Observed ratios are Bijvoet difference ratios (diagonal elements) at each wavelength (values in parentheses are for centric reflections) and dispersive difference ratios (off-diagonal elements) between pairs of wavelengths. $R(F_A)$ is the residual between the calculated structure factors based on the Se positions and those obtained from the MAD analysis. $\Delta(\Delta\phi)$ is the average difference between independent determinations of $\Delta\phi$ from the MAD analysis[21].

logues of p38, named p38β and p38γ, were identified which share about 70% sequence identity with p38[18,19].

Overall Structure

In order to understand the structural basis for the potency and specificity of the pyridinyl-imidazole CSAID inhibitors, and to compare the structures of two different MAP kinases, we determined the crystal structure of human p38 MAP kinase (CSBP2)[14] in complex with a 3'-iodo pyridinyl-imidazole inhibitor derived from the CSAID SB 203580[17,20] (Fig. 1). SB 203580 is highly potent against the p38 MAP kinase, with a K_d of about 40 nM[14]. The iodine atom was introduced to facilitate the identification of inhibitor binding sites; the iodinated compounds have similar potencies against the kinase as the parent SB 203580 compound (L.T. *et al.*, unpublished data). The crystal structure was determined by a combination of molecular replacement using ERK2 as the model and seleno-methionyl multiple wavelength anomalous diffraction (MAD)[21] (Table 1; see Methods). The current atomic model contains residues 5–117, 123–169 and 185–352 of the kinase, three 3'-iodo inhibitor molecules, and 195 water molecules.

The kinase is in an open conformation[8,22], and is in the inactive (unphosphorylated) state (Fig. 2*a*). A total of 279 equivalent Cα atoms between p38 and ERK2[8], located within 2.5 Å, could be superimposed between the two structures, giving an r.m.s. distance of 1.4 Å. The ERK2 structure is also in the inactive, unphosphorylated state. The relative positions of the N- and C-terminal lobes of p38 MAP kinase are similar to those of ERK2. In contrast, the structure of apo p38 MAP kinase[23] shows a large difference in the positions of the two domains relative to ERK2. Residues in helix α_C, the glycine-rich loop (residues 30–38), loop L12, helices α_{1L14} and α_{2L14}, and loop L16 show distinct differences between p38 and ERK2 (Fig. 2*b*). Some of these differences could be caused by inhibitor binding (see below). Residues 170–184, from β9 and the beginning of loop L12, is disordered in the current structure. This segment, a portion of which was ordered in the apo enzyme structure[23], contains the activation motif of p38 (TGY). The conformation of residues in this segment[23] in the apo enzyme is significantly different from the equivalent residues in ERK2, as the activation segment of p38 MAP kinase is six residues shorter. In addition, residues 1–4 (and the N-terminal His-tag), 118–122, and 353–360 are disordered and not included in the current atomic model.

Inhibitor binding mode and specificity

Three inhibitor molecules were found to be associated with each p38 MAP kinase molecule in the crystal. The first CSAID molecule is bound in the ATP pocket, inserted into the deep cleft

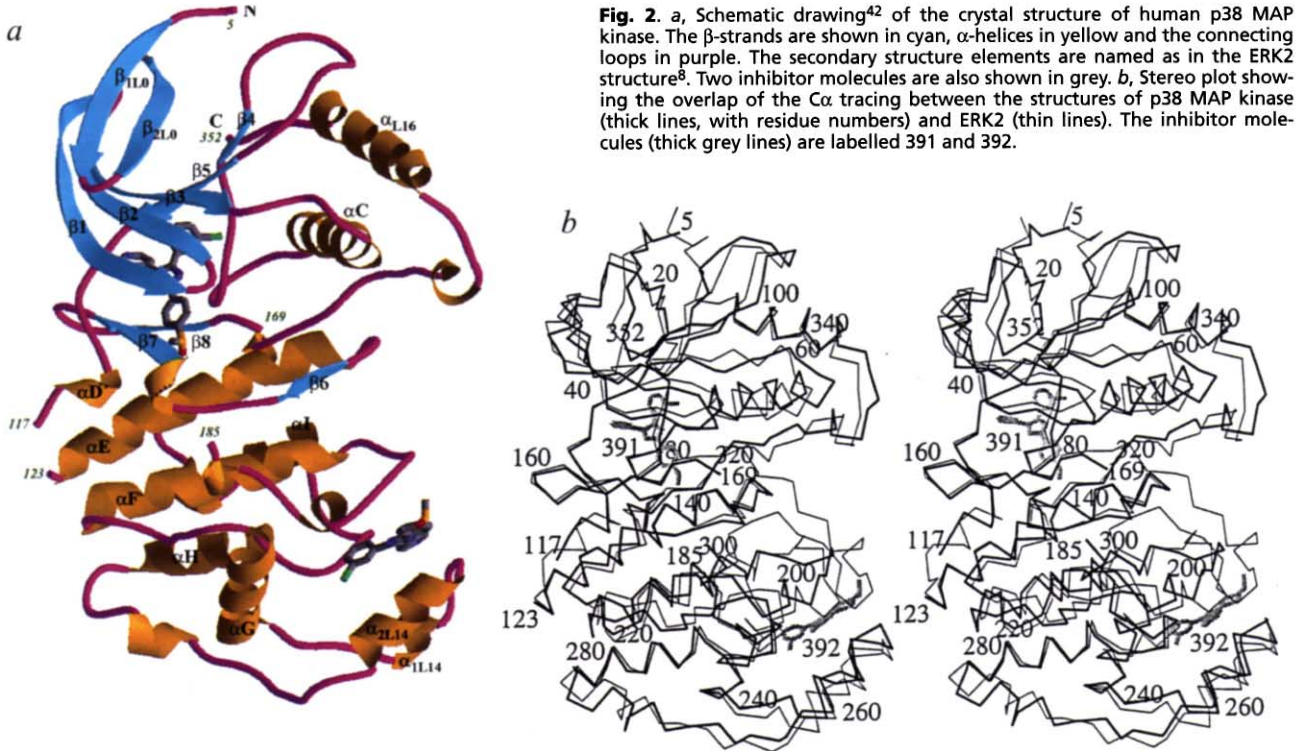

Fig. 2. *a*, Schematic drawing[42] of the crystal structure of human p38 MAP kinase. The β-strands are shown in cyan, α-helices in yellow and the connecting loops in purple. The secondary structure elements are named as in the ERK2 structure[8]. Two inhibitor molecules are also shown in grey. *b*, Stereo plot showing the overlap of the Cα tracing between the structures of p38 MAP kinase (thick lines, with residue numbers) and ERK2 (thin lines). The inhibitor molecules (thick grey lines) are labelled 391 and 392.

between the two lobes of the kinase (Fig. 3*a*,*b*). The binding mode is similar to that of ATP[5–10], although there are also significant differences (Fig. 3*c*). The pyridyl ring of the inhibitor occupies a position similar to that of the six-membered ring of the adenine base of ATP. A hydrogen-bond between the pyridyl ring nitrogen and the main chain amido group of residue 109 is analogous to the interaction observed from the N1 atom of the adenine base[5–10]. The other conserved hydrogen-bond, from the N6 atom of adenine to a backbone carbonyl group (of residue 107 in p38 MAP kinase), is however absent in this structure. The imidazole ring is in the general location of the five-membered ring of adenine, with a water molecule hydrogen-bonded to each of its ring nitrogens. The 3'-iodophenyl group interacts with the main chain of residues 51–53 and 104–106, and the side chains of Val 38, Ala 51, Thr 106 and the aliphatic portion of the conserved Lys 53, which forms the conserved ion pair with Glu 71. The iodine atom is in a somewhat hydrophobic pocket, formed by Leu 75, Leu 86, Leu 104 and the Lys 53–Glu 71 ion pair. The *p*-methylsulphinylphenyl group occupies a position similar to the phosphate groups of the ATP. It is partly exposed to solvent and has weaker electron density (Fig. 1*b*), suggesting that it may be flexible. The side chain of Tyr 35, from the glycine-rich loop which binds the phosphates of ATP, is situated above this phenyl ring in the current atomic model. However, the electron density for this side chain is rather weak, suggesting that any interactions it may have with the inhibitor are probably weak as well.

The crystal structure provides satisfactory explanations for many of the observed structure-activity relationships of this class of inhibitors[24,25]. When the nitrogen atom in the pyridyl ring was moved from the *para*-position to the *ortho*- or *meta*-position, the potencies of the inhibitors decreased by more than 500-fold. This confirms the importance of the hydrogen-bond as observed in the crystal structure. The *p*-methylsulphinylphenyl group has weak electron density in the crystal structure analysis, suggesting that it may only have weak interactions with the kinase. Removal of this entire group only led to a threefold loss in inhibitory activity. It was also found that substitutions at the 2-position of the imidazole ring could be moved to the N1 atom without significantly affecting the potency of the inhibitors. The crystal structure shows that the N1 atom is exposed to solvent, and substituents at this position will likely be placed near the binding site for the ribose ring of ATP (Fig. 3*c*).

Structural differences between the p38 MAP kinase and the closely-related ERK2 may help explain the specificity of the pyridinyl-imidazole inhibitors. In comparing the binding mode of the inhibitor with that of ATP, it is clear that the 4-phenyl ring is located in a part of the binding pocket that is not utilized by ATP. Hence, it is tempting to speculate that this phenyl ring is the major determinant for the specificity of these inhibitors against p38 MAP kinase. Near this phenyl ring, one difference is the replacement of Thr 106 in p38 by Gln 103 in ERK2. The extra bulk introduced by the larger Gln side chain may interfere with the binding of this phenyl ring of the inhibitor by ERK (Fig. 3*d*). This is partly supported by the observation that the Gln 103 side chain of ERK2 could be in a steric clash with the 4-phenyl ring of the inhibitor (Fig. 3*d*). This residue is a Thr in p38β, which is sensitive to these inhibitors[18], and is replaced by a larger residue in many other kinases[26]. However, this residue is also a Thr in *raf*, which is insensitive to these inhibitors[17], and the homologue p38γ has a bulky Met at this position, yet is sensitive to these inhibitors[19].

There are other structural differences in this region of the binding pocket. A difference in the conformation of helix α_C in p38 affects the location of the Lys 53–Glu 71 ion pair. The Lys 52 side chain in the ERK2 structure (equivalent of Lys 53 in p38) would be in steric clash with the 4-phenyl ring (Fig. 3*d*). This conformational change in helix α_C may be an essential difference between p38 and ERK2. There is an one-residue deletion in ERK2 in the loop leading to helix α_C which may be in part responsible for the difference in conformation. This conforma-

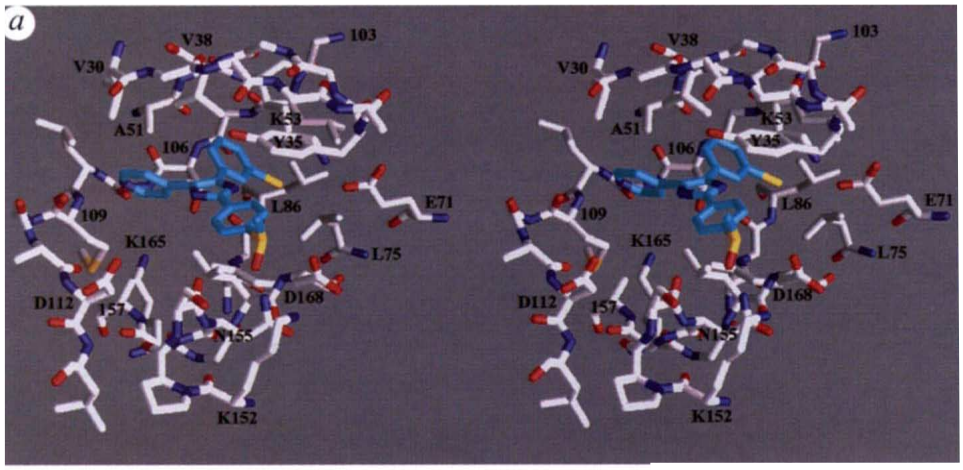

Fig. 3 *a*, Stereo plot[43] showing detailed interactions between the 3'-iodo inhibitor (cyan) and the ATP binding pocket (white) of the p38 MAP kinase. Oxygen atoms are red, nitrogens blue, sulphurs and iodine yellow. Water molecules and some of the side chains for the residues not involved in inhibitor binding are not shown. *b*, Molecular surface of p38 MAP kinase near the inhibitor in the ATP binding pocket, coloured red for negatively-charged regions and blue for positively charged regions. The inhibitor molecule is also shown. *c*, Superposition of the binding modes for the 3'-iodo inhibitor (cyan) and ATP (in purple for carbon atoms), as observed in the structure of casein kinase[9]. The optimal structural alignment may be slightly different from the figure shown here, as the relative positions of the two lobes in casein kinase are different than those of p38. *d*. Stereo plot[43] showing the structural superposition of p38 MAP kinase (white, black numbers) with 3'-iodo inhibitor (cyan), and ERK2 (green with green numbers), in the ATP binding pocket. Lys 52 and Gln 103 of ERK2 are in a steric clash with the 3'-iodophenyl ring of the inhibitor. The Lys-Glu ion pairs are located in different positions between the two structures due to a difference in the position of helix α_C.

tional difference may also be induced by the 3'-iodophenyl ring of the inhibitor as it is located near helix α_C. Structural differences in other areas of the binding pocket may contribute to specificity as well. The glycine-rich loop is closer to the inhibitor and the C-terminal lobe in the p38 structure (Fig. 3*d*) than that in ERK2. However, it is possible that this conformational difference is induced by the inhibitor as the glycine-rich loop is rather flexible. There are also other, largely conservative, amino acid differences between p38 and ERK2 (V30I, L104I, A157L, L167C) in this binding pocket; the amino acid changes A157L and L167C are compensatory in nature (Fig. 3*d*). In summary, both conformational differences and side chain substitutions may contribute to the specificity of the inhibitor.

Crystal structures of inhibitor complexes of cyclin-dependent protein kinase 2 (CDK2)[27,28] and casein kinase-1 (CK1)[29] have been reported. In the structure of CDK2 in complex with the inhibitor olomoucine, a phenyl ring of the inhibitor is bound in a region which is not utilized by ATP. This is similar to the binding of the 4-phenyl group of the inhibitor in the current study, although the positions of the phenyl rings in the two structures are very different. In inhibitor complexes of both CDK2 and CK1, a hydrogen bond was observed between the inhibitor and the protein, equivalent to the one from the pyridyl ring nitrogen in the current structure. This hydrogen bond may therefore be an important component in the binding of inhibitors to protein kinases. However, the CDK2 and CK1 inhibitors used in the structural studies are selective inhibitors, as they also inhibit other kinases. Moreover, they have relatively weaker potency, with IC_{50} or K_i in the micromolar range. Therefore, this structure of p38 MAP kinase inhibitor complex represents the first report of a protein kinase in complex with a highly potent and highly specific inhibitor.

A second binding site of unknown function

A second CSAID inhibitor molecule in the

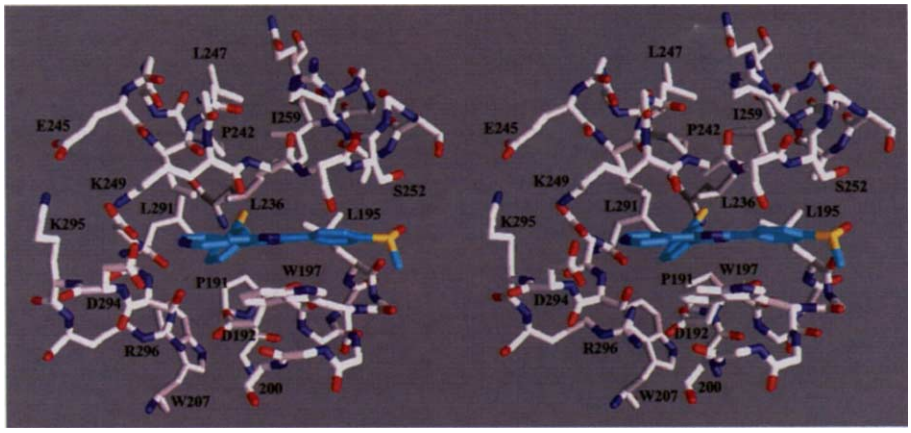

Fig. 4 Stereo plot[43] showing the detailed interactions between the 3'-iodo inhibitor in the second binding pocket (the I-pocket) of the p38 MAP kinase. The colouring scheme is the same as for Fig. 3*a*.

structure is bound in a pocket that is far removed (~30 Å) from the ATP pocket (Fig. 2*a*). This inhibitor is located in a deep groove (Fig. 4) between the conserved core of the C-terminal lobe and the major insert after helix α_G that is present in the MAP kinases (helices α_{1L14} and α_{2L14})[8] and CDKs[7]. One face of the inhibitor is π-stacked against the side chain of Trp 197 from loop L12. It also interacts with the Glu 192–Arg 296 ion pair that is conserved in most protein kinases (Glu 208–Arg 280 in cyclic AMP-dependent protein kinase). A large conformational difference is observed for residues in this region between p38 (residues 194–200) and ERK2 (Fig. 2*a*). The other face of the inhibitor interacts with the main chain atoms of residues 249–252 (the connecting loop between α_{1L14} and α_{2L14}) (Fig. 2*a*, 4). The pyridyl ring nitrogen is 2.8 Å from the side chain carboxylate group of Asp 294, which is also involved in a network of ion-pair interactions with Glu 245, Asp 292, Lys 295 and several water molecules. A water molecule is associated with the exposed N1 atom of the imidazole. The iodine atom is tightly bound by a highly hydrophobic pocket, formed by the side chains of Pro 191, Leu 195, Leu 232, Leu 236, Pro 242, Leu 246, Leu 247, Ile 250, Ile 259 and Leu 291 (Fig. 4).

This pocket therefore may have high affinity for the inhibitor. However, in the structures of the parent compound SB 203580 (3.0 Å resolution) and the 4'-iodo compound (2.0 Å resolution), only the ATP pocket is occupied and this second pocket is empty (L. T. *et al.*, unpublished data); possibly the 3'-iodo compound is bound in this pocket due to the strong interactions between the iodine atom and the hydrophobic pocket (hence we propose the name I-pocket for this second binding site). The inhibitor is present at 10-fold molar excess in the crystallization condition, corresponding to a concentration of about 1.4 mM[20]. This is significantly higher than the potency of about 40nM of this inhibitor[14] against the p38 MAP kinase. The significance of this site for the inhibition of the biological activity of p38 MAP kinase is unclear. The amino-acid differences between CSBP1 and CSBP2 occur near this region (residues 228–254)[14]. In the CDKs, residues near this region are important for the binding of another protein, although the biological function of this interaction is still unknown[30,31].

A third inhibitor molecule is only weakly bound, trapped at the interface between two neighbouring p38 molecules in the crystal. Therefore, its presence is most likely due to crystal packing.

Specificity and drug design

Several classes of inhibitors that are selective or specific against individual protein Ser/Thr-kinases[14,29] and especially protein Tyr-kinases[32,33] have been reported. The current structural study shows that it is possible to achieve stringent specificity by utilizing the ATP binding pocket, which is present in most of these enzymes. Such inhibitors would generally contain a portion that roughly mimics the ATP molecule, and a portion that protrudes away from the ATP envelope to achieve specificity. A hydrogen-bond, equivalent to that from the N1 atom and/or the N6 atom of adenine, may be important in conferring additional potency and specificity. It is possible that some of the active-site inhibitors that have been reported achieve their specificity through this mechanism. However, other mechanisms of achieving specificity using this ATP binding region may be possible as well.

The regulation of many cellular processes depends critically on the phosphorylation states of the controlling proteins. Protein kinases and phosphatases, which modulate these phosphorylation states, therefore play crucial roles in regulating cellular processes. The selective inhibition of specific kinases (or phosphatases) represents an attractive approach for the pharmaceutical intervention of various disease states. Inhibitors of p38 MAP kinase, for example, can reduce the host inflammatory response[14,16] and may prove efficacious towards disease states such as rheumatoid arthritis[34]. The structural information obtained from this and other studies will help in the design and optimization of specific inhibitors against protein kinases.

Methods

The cloning[14], expression, purification and crystallization of human p38 MAP kinase have been described[20]. Crystals were obtained in the presence of three different pyridinyl-imidazole inhibitors[17] (Fig. 1). X-ray diffraction data on the complex with the 3'-iodo inhibitor were collected at cryo-temperature at the X4A beamline at the Brookhaven National Laboratory on the native protein (2.0 Å resolution) and the seleno-methionyl protein (2.7 Å). Four wavelengths were used to collect the MAD data on the seleno-methionyl protein—0.9919 Å (λ1), 0.9793 Å (λ2), 0.9792 Å (λ3), and 0.9724 Å (λ4). The diffraction images were processed with DENZO[35], and the data processing statistics are summarized in Table 1. The native and the seleno-methionyl crystals are isomorphous and belong to space group $P2_12_12_1$, with cell dimensions of a=65.1 Å, b=74.3 Å and c=77.9 Å for the crystal of the native protein. There is one molecule of the kinase in the asymmetric unit.

The atomic model of ERK2[8] was used to provide an initial solution of the structure of p38 MAP kinase by a combined molecular replacement protocol[36] as implemented in the REPLACE package[37]. This initial solution was critical in locating the selenium atoms based on the seleno-methionyl MAD data. The ERK2 atomic model was modified by truncating to Ala those residues that have large sequence differences and deleting those loops that have significant insertions or deletions between ERK2 and p38. The N- and C-terminal lobes were used separately as models for molecular replacement, with the orientation and position of the C-terminal lobe being determined first. The phases from this molecular replacement solution were used in an anomalous difference map for the seleno-methionyl data, which revealed four out of the 10 expected Se positions. The MAD data on the seleno-methionyl protein were used to derive the protein phases, using both the MADSYS package[21] and X-PLOR[38]. The quality of the MAD data set, and consequently the MAD phasing statistics are very poor (Table 1). The

phases were improved by solvent-flattening[39] and used to calculate another anomalous difference map, which revealed two additional Se sites and what turned out to be the iodine atom on the inhibitor in the second binding pocket. The remaining four selenium sites are probably disordered. After further MAD phasing and solvent-flattening, the ERK2 atomic model was modified with the program FRODO[40] to fit the electron density and the sequence of p38 MAP kinase.

The structure was refined with X-PLOR[38] against the data set on the native protein to 2.0 Å resolution. Simulated-annealing omit refinements were carried out throughout the entire sequence, leaving out 20 residues at a time, to ascertain the conformation of the atomic model. Residues Asn 14 and Lys 15 were modelled as Ala residues due to lack of density and assume unfavourable main chain conformations. Two other residues (Ser 95 and Asp 168, both in exposed surface loops) are in high energy regions of the Ramachandran plot. Two inhibitor molecules were found in the initial difference maps, recognized by the strong electron density for the iodine atoms. After further refinement, a third inhibitor molecule was found, weakly bound at the crystal packing interface. Water molecules were identified from peaks in the difference electron density maps that were located near possible hydrogen-bond donors or acceptors. The temperature factor values for the water molecules range between 20–50 Å^2, with an average value of 38 Å^2. The average temperature factor value for the protein atoms is 28 Å^2. The individual temperature factors were tightly restrained during the refinement. Coordinates have been deposited in the Brookhaven Protein Data Bank (ID code 1IAN)

Acknowledgements

We thank E. Goldsmith for kindly providing the atomic model of ERK2; C. Ogata and D. Cook for help with the data collection at the X4A beamline at the Brookhaven National Laboratory; W. Hendrickson and H. Wu for the MADSYS package; A. Brünger for a pre-release version of X-Plor 4.0; J. Hopkins and W. Davidson for characterization of the protein samples by tryptic digest and mass spectrometry.

Received 6 December 1996; Accepted 27 February 1997

1. Seger, R. & Krebs, E. G. The MAPK signaling cascade. *FASEB J.* **9**, 726-735, (1995).
2. Cobb, M. H. & Goldsmith, E. J. How MAP kinases are regulated. *J. Biol. Chem.* **270**, 14843-14846 (1995).
3. Johnson, L. N., Noble, M. E. M. & Owen, D. J. Active and inactive protein kinases: Structural basis for regulation. *Cell* **85**, 149-158, (1996).
4. Taylor, S. S. & Radzio-Andzelm, E. Three protein kinase structures define a common motif. *Structure*, **2**, 345-355 (1994).
5. Zheng, J. *et al.* Crystal structure of the catalytic subunit of cAMP-dependent protein kinase complexed with MgATP and peptide inhibitor. *Biochem.* **32**, 2154-2161(1993).
6. Bossemeyer, D., Engh, R. A., Kinzel, V., Ponstingl, H. & Huber, R. Phosphotransferase and substrate binding mechanism of the cAMP-dependent protein kinase catalytic subunit from porcine heart as deduced from the 2.0Å structure of the complex with Mn^{2+} adenylyl imidodiphosphate and inhibitor peptide PKI(5-24). *EMBO J.* **12**, 849-859 (1993).
7. De Bondt, H. L. *et al.* Crystal structure of cyclin-dependent kinase 2. *Nature* **363**, 595-602 (1993).
8. Zhang, F., Strand, A., Robbins, D., Cobb, M. H. & Goldsmith, E. J. Atomic structure of the MAP kinase ERK2 at 2.3Å resolution. *Nature* **367**, 704-711 (1994).
9. Xu, R.-M., Carmel, G., Sweet, R. M., Kuret, J. & Cheng, X. Crystal structure of casein kinase-1, a phosphate-directed protein kinase. *EMBO J.* **14**, 1015-1023 (1995).
10. Owen, D. J., Noble, M. E. M., Garman, E. F., Papageorgiou, A. C. & Johnson, L. N. Two structures of the catalytic domain of phosphorylase kinase: an active protein kinase complexed with substrate analogue and product. *Structure* **3**, 467-482 (1995).
11. Han, J., Lee, J.-D., Bibbs, L. & Ulevitch, R. J. A MAP kinase targeted by endotoxin and hyperosmolarity in mammalian cells. *Science* **265**, 808-811 (1994).
12. Rouse, J. *et al.* A novel kinase cascade triggered by stress and heat shock that stimulates MAPKAP kinase-2 and phosphorylation of the small heat shock proteins. *Cell* **78**, 1027-1037 (1994).
13. Freshney, N. W. *et al.* Interleukin-1 activates a novel protein kinase cascade that results in the phosphorylation of Hsp27. *Cell* **78**, 1039-1049 (1994).
14. Lee, J. C. *et al.* A protein kinase involved in the regulation of inflammatory cytokine biosynthesis. *Nature* **372**, 739-746 (1994).
15. Raingeaud, J. *et al.* Pro-inflammatory cytokines and environmental stress cause p38 mitogen-activated protein kinase activation by dual phosphorylation on tyrosine and threonine. *J. Biol. Chem.* **270**, 7420-7426 (1995).
16. Lee, J. C. *et al.* Bicyclic imidazoles as a novel class of cytokine biosynthesis inhibitors. *Ann. N.Y. Acad. Sci.* **696** 149-170 (1993).
17. Cuenda, A. *et al.* SB 203580 is a specific inhibitor of a MAP kinase homologue which is stimulated by cellular stresses and interleukin-1. *FEBS Lett.* **364**, 229-233 (1995).
18. Jiang, Y. *et al.* Characterization of the structure and function of a new mitogen-activated protein kinase (p38β). *J. Biol. Chem.* **271**, 17920-17926 (1996).
19. Li, Z., Jiang, Y., Ulevitch, R. J. & Han, J. The primary structure of p38γ: A new member of p38 group of MAP kinases. *Biochem. Biophys. Res. Commun.* **228**, 334-340 (1996).
20. Pav, S. *et al.* Crystallization and preliminary crystallographic analysis of recombinant human p38 MAP kinase. *Protein Sci.* **6**, 242-245 (1997).
21. Hendrickson, W. A. Determination of macromolecular structures from anomalous diffraction of synchrotron radiation. *Science* **254**, 51-58 (1991).
22. Cox, S., Radzio-Andzelm, E. & Taylor, S. S. Domain movements in protein kinases. *Curr. Opin. Struct. Biol.* **4**, 893-901 (1994).
23. Wilson, K. P. *et al.* Crystal structure of p38 mitogen-activated protein kinase. *J. Biol. Chem.* **271**, 27696-27700 (1996).
24. Gallagher, T. F. *et al.* 2,4,5-triarylimidazole inhibitors of IL-1 biosynthesis. *Bioorg. Med. Chem. Lett.* **5**, 1171-1176 (1995).
25. Boehm, J. C. *et al.* 1-substituted 4-aryl-5-pyridinylimidazoles: A new class of cytokine suppressive drugs with low 5-lipoxygenase and cyclooxygenase inhibitory potency. *J. Med. Chem.* **39**, 3929-3937 (1996).
26. Hanks, S. K., Quinn, A. M. & Hunter, T. The protein kinase family: Conserved features and deduced phylogeny of the catalytic domains. *Science* **241**, 42-52 (1988).
27. Schulze-Gahmen, U. *et al.* Multiple modes of ligand recognition: Crystal structures of cyclin-dependent protein kinase 2 in complex with ATP and two inhibitors, olomoucine and isopentenyladenine. *Proteins* **22**, 378-391 (1995).
28. De Azevedo Jr., W. F. *et al.* Structural basis for specificity and potency of a flavonoid inhibitor of human CDK2, a cell cycle kinase. *Proc. Natl. Acad. Sci. USA* **83**, 2735-2740 (1996).
29. Xu, R.-M., Carmel, G., Kuret, J. & Cheng, X. Structural basis for selectivity of the isoquinoline sulfonamide family of protein kinase inhibitors. *Proc. Natl. Acad. Sci. USA* **93**, 6308-6313 (1996).
30. Bourne, Y. *et al.* Crystal structure and mutational analysis of the human CDK2 kinase complex with cell cycle-regulatory protein CksHs1. *Cell* **84**, 863-874 (1996).
31. Pines, J. Cell cycle: reaching for a role for the Cks proteins. *Curr. Biol.* **6**, 1399-1402 (1996).
32. Fry, D. W. & Bridges, A. J. Inhibitors of protein tyrosine kinases. *Curr. Opin. Biotech.* **6**, 662-667 (1995).
33. Hanke, J. H. *et al.* Discovery of a novel, potent, and src family-selective tyrosine kinase inhibitor. *J. Biol. Chem.* **271**, 695-701 (1996).
34. Badger, A. M. *et al.* Pharmacological profile of SB 203580, a selective inhibitor of cytokine suppressive binding protein/p38 kinase, in animal models of arthritis, bone resorption, endotoxin shock and immune function. *J. Pharm. Exp. Therapeutics* **279**, 1453-1461 (1996).
35. Otwinowski, Z. In *Data Collection and Processing* (Sawyer, L., Isaacs, N. & Bailey, S., eds.) 56-62. (SERC Daresbury Laboratory) (1993).
36. Tong, L. Combined molecular replacement. *Acta Cryst.* **A52**, 782-784 (1996).
37. Tong, L. Replace: A suite of computer programs for molecular-replacement calculations. *J. Appl. Crystallogr.* **26**, 748-751 (1993).
38. Brünger, A. T.*The X-PLOR manual, version 3.0.* Yale University, New Haven, CT. (1992).
39. Wang, B. C. Resolution of phase ambiguity in macromolecular crystallography. *Meth. Enzymol.* **115**, 90-112 (1985).
40. Jones, T. A. A graphics model building and refinement system for macromolecules. *J. Appl. Crystallogr.* **11**, 268-272 (1978).
41. Brünger, A. T. Free R value: a novel statistical quantity for assessing the accuracy of crystal structures. *Nature* **355**, 472-475 (1992).
42. Carson, M. Ribbon models of macromolecules. *J. Mol. Graphics*, **5**, 103-106 (1987).
43. Nicholls, A., Sharp, K. A. & Honig, B. Protein folding and association: insights from the interfacial and thermodynamic properties of hydrocarbons. *Proteins* **11**, 281-296 (1991).